

# Reasoning in machine vision: learning to think fast and slow

Shaheer U. Saeed<sup>1,2,3\*</sup>, Yipei Wang<sup>1,2,3</sup>, Veeru Kasivisvanathan<sup>4</sup>,  
Brian R. Davidson<sup>4</sup>, Matthew J. Clarkson<sup>1,2,3</sup>, Yipeng Hu<sup>1,2,3</sup>,  
Daniel C. Alexander<sup>1,3</sup>

<sup>1</sup>UCL Hawkes Institute, University College London, UK

<sup>2</sup>Department of Medical Physics and Biomedical Engineering, University  
College London, UK

<sup>3</sup>Department of Computer Science, University College London, UK

<sup>4</sup>Division of Surgery and Interventional Sciences, University College London, UK

\*Correspondence e-mail: shaheer.saeed.17@ucl.ac.uk

## Abstract

Reasoning is a hallmark of human intelligence, enabling adaptive decision-making in complex and unfamiliar scenarios. In contrast, machine intelligence remains bound to training data, lacking the ability to dynamically refine solutions at inference time. While some recent advances have explored reasoning in machines, these efforts are largely limited to verbal domains such as mathematical problem-solving, where explicit rules govern step-by-step reasoning. Other critical real-world tasks - including visual perception, spatial reasoning, and radiological diagnosis - require non-verbal reasoning, which remains an open challenge. Here we present a novel learning paradigm that enables machine reasoning in vision by allowing performance improvement with increasing thinking time (inference-time compute), even under conditions where labelled data is very limited. Inspired by dual-process theories of human cognition in psychology, our approach integrates a fast-thinking System I module for familiar tasks, with a slow-thinking System II module that iteratively refines solutions using self-play reinforcement learning. This paradigm mimics human reasoning by proposing, competing over, and refining solutions in data-scarce scenarios. We demonstrate superior performance through extended thinking time, compared not only to large-scale supervised learning but also foundation models and even human experts, in real-world vision tasks. These tasks include computer-vision benchmarks and cancer localisation on medical images across five organs, showcasing transformative potential for non-verbal machine reasoning.

## Introduction

### Rethinking machine cognition - beyond data-driven learning

Human cognition excels at new tasks with minimal prior experience through reasoning, by dedicating cognitive resources, such as extended thinking time, to planning and strategising [1–3]. This is enabled by dual-process human cognition [1]: System I enables fast, intuitive decisions based on prior experience, while System II facilitates slow, deliberate reasoning, especially in unfamiliar scenarios. Current deep learning systems lack the capacity to perform reasoning or System II thinking [4, 5], relying heavily on extensive human-labelled data or repeated task exposure to perform well in familiar scenarios [6]. While such data-driven experience yields strong performance within the scope of training data, these systems falter when labelled data is insufficient to represent new tasks [6–8]. Here, we propose a novel algorithm which enables System II thinking and equips machines with the ability to improve performance with increasing thinking time (inference-time computation), rather than resorting to additional labelled data.

### Two systems of human cognition and their transition in psychology

Theories from cognitive psychology have observed that fast and intuitive System I thinking allows humans to make confident decisions for familiar tasks, despite unclear immediate justifications [1–3]. In contrast, System II thinking consumes cognitive resources at the time of the decision-making [1]. For instance, a beginner chess player can reason about potential moves, plan and develop complex strategies using only the game rules, despite limited gameplay experience. One key cognitive resource consumed in such processes is thinking time and its mechanisms include comparison of hypothetical scenarios, considering long-term outcomes in greater detail, and breaking problems into simpler parts before solving them [1, 5]. Attention is another critical cognitive resource [1], which can be consumed through mechanisms such as filtering out irrelevant information (e.g., ignoring background speech while reading) [9]. Consuming these resources allows improvements in decision quality, which is an ability considered unique to humans [5].

With experience, humans can transition tasks from slow, deliberate System II to much faster System I thinking [3] e.g., the ability of experienced chess players to execute strategies more quickly and instinctively as their experience grows. The interplay between fast and slow thinking allows versatility in human cognition, which is capable of handling both familiar and unfamiliar scenarios, unlike conventional machine cognition in deep learning systems, which arguably only operates in a fast, experience-driven System I paradigm. We present examples, in Fig. 1, showcasing

tasks typically solved by System I and System II thinking, along with tasks that have likely transitioned between the two.



Is an egg present?

(a) The answer to this question may be apparent intuitively, even without clear reasons at first. If asked, you might justify it with explanations like seeing the egg shell or the shape. However, justifications are likely only post-hoc. This demonstrates fast, implicit, and unconscious System I thinking, where no explicit reasons are apparent prior to the decision itself.



How many eggs?

(b) Solving this manually requires slow and conscious thought. You might estimate the answer by multiplying eggs in a row and column, improving accuracy with more time, or count consciously. At the end, the justification for how you obtained the answer would be clear. This demonstrates slow, explicit System II thinking. Generated using DALLE-2.



How many eggs?

(c) This problem is likely quickly solved, possibly without any explicit counting, due to frequent encounters with similar six-egg cartons in the past. This demonstrates a transition, where problems initially requiring deliberate thought (System II), with experience, become automatic and unconscious when committed to memory (System I).

**Fig. 1:** Examples illustrating System I and System II cognitive processes.

## Single-system machine cognition and its shortfalls

Supervised deep learning algorithms are highly dependent on large labelled data sets and lack mechanisms to improve by extending thinking time (inference-time compute) [4, 5, 8], or handle scenarios beyond the training distribution [10]. Approaches like few-shot learning [11–13] and foundation models [14–17] aim to use task-specific data more efficiently. However, they exhibit fixed, often linear, computational complexity with respect to data availability and the only viable mechanism to improve performance further is to train with more human-labelled data [18–20].

Developing System II capabilities in machines, allowing performance improvement with an increase in thinking time, is therefore crucial, not only as a step towards emulating biological intelligence but also to overcoming practical challenges stemming from the cost and scarcity of labelled data [10].

## Progress towards enabling System II capabilities in machines

Prior work on implementing System II thinking in machine inference, through extended thinking (computation) time, has focused on constrained and restrictive domains, such as board games [4]. These approaches modelled System I and System II separately, without explicit modelling of the connection between the two. In these works the System II slow-thinking process is implemented as an exhaustive, structured, random or guided search over promising moves, as a mechanism to consume

thinking time [4, 21, 22]. While these approaches improve performance by extending thinking time without requiring additional task-specific data, they are limited to scenarios with manageable search spaces or to specialised domains such as language [23–27]. Recent work has also modelled System II thinking using a reinforcement learning process guided by a reward signal. However, these remain limited to the language domain, relying largely on verifiable tasks such as mathematics problems, using rule-based verification of final outcomes or intermediate steps, to generate rewards [28–31], sometimes involving human observers [32, 33].

Another type of cognitive resource in machines is attention which may also be considered as a model for System II thinking, although has been explored only in the context of natural language applications [34]. Techniques such as ‘divide-and-conquer’ [35] and ‘chain-of-thought’ [36] break down complex tasks into parts before solving them. These mechanisms enable neural networks to improve through a refinement of their inputs, either guided by a human observer [36] or through iterative guided refinements of their own inputs which also increases inference-time compute [34]. However, they remain limited to sequential query-response domains, such as large language models trained/fine-tuned on paired question-and-answer chat-based data, owing to the ease of verifying correctness in such domains. Arguably, attention mechanisms common in language applications do not model System II thinking [37–40], as they do not possess an ability to dynamically alter behaviours for new samples or tasks, with attention often learnt based on task-specific experience itself.

Most of this previous work has focused on emulating verbal reasoning, however, non-verbal or visual reasoning has potential to enhance various applications including robotics, medical diagnostics, and astronomy. Many real-world tasks require reasoning about spatial relationships, object boundaries, and patterns without relying on language-based logic. In medical imaging, for instance, clinicians identify and interpret complex visual features to diagnose diseases—an inherently non-verbal reasoning process. Developing systems capable of such non-verbal reasoning is essential for advancing machine intelligence beyond text-based tasks and into broader, high-impact applications.

The main hindrance in implementing reasoning for vision tasks, such as identifying object boundaries, stems from the fact that solutions are often more complex with much higher-dimensional solution spaces. The methods above do not extend naturally to explore such spaces, which often have nuanced solutions with multiple nearly-correct outcomes. This makes development of the verification-based rewards, challenging in such domains. For example, even in a simple real-world 2D image segmentation to localise objects, the solution space is astronomically large, far beyond the computational capacity for exhaustive search, or for manual design of rule-based verification strategies.<sup>1, 2</sup> Some efforts allow improved performance as a result of slow thinking [41, 42] but operate with fixed thinking periods, limiting their scalability, with further performance improvements not possible with an increase in thinking time. Thus

---

<sup>1</sup>Assuming a  $512 \times 512$  image with a single object, there are  $\sum_{r=0}^{512 \times 512} \frac{(512 \times 512)!}{r!((512 \times 512) - r)!} \gg 10^{1000}$  possibilities

<sup>2</sup>For chess, 16 pieces per side, each with 16 moves, there are  $\frac{16!}{1!(16-1)!} \times \frac{16!}{1!(16-1)!} = 256$  possibilities per-move

modelling of the reasoning enabled by System II thinking remains uncharted in the context of vision applications.

## System II machine cognition: an auto-competing mechanism

We propose to emulate human dual-process cognition in deep learning algorithms through two interconnected modules: 1) the System I module, trained on human-labelled data across various tasks, to produce fast solutions; and 2) the System II module, which allows for refinement and optimisation of solutions produced by the System I module. Even in data-limited scenarios, this framework allows performance improvements with added inference-time compute. Additionally, the System II module, after fully refining the solutions, feeds back to the System I module to improve its fast solutions for subsequent data, reducing time required for refinement in the System II module. An overview of the described method, compared to conventional approaches, is illustrated in Fig. 2.

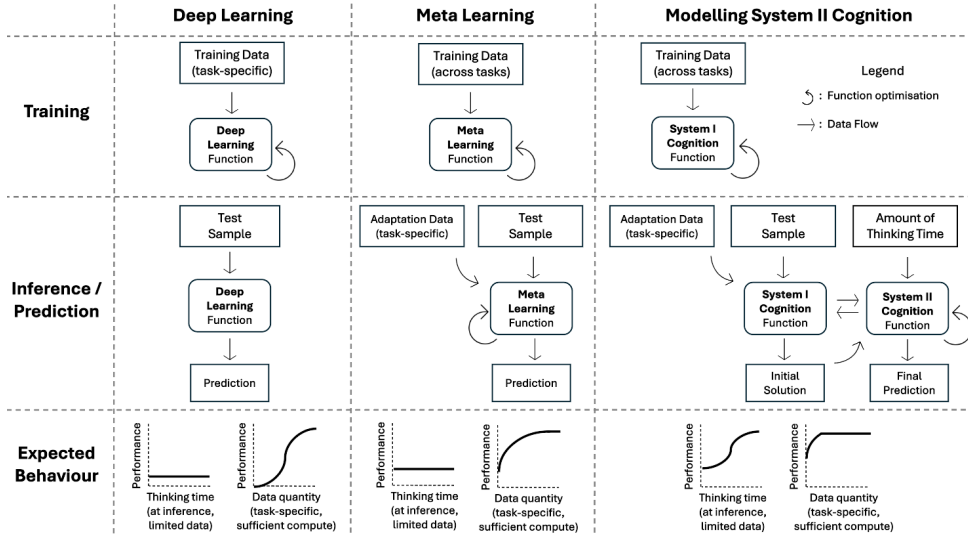


**Fig. 2:** Different learning strategies are compared: deep learning for a single forward pass prediction, meta-learning for adapting to new tasks (akin to fine-tuning pre-trained foundation models), and the proposed System II cognition for allowing inference-time compute. Details of these are described in text.

Here we demonstrate a System I module that consists of two neural networks trained adversarially [43] across a variety of tasks, using human-labelled data. This mimics the experience-driven System I thinking in human psychology. The first network in this module is a task-predictor, which produces a solution (such as localising an object) given an input image. The second network is a distribution-discriminator which

measures the likelihood of solutions being correct, by leveraging pre-learned knowledge from a variety of human-labelled data across multiple tasks. In the adversarial training, human labels are regarded as correct solutions and task-predictor solutions are regarded as incorrect. The aim during training is for the task-predictor to produce solutions close to human labels, and the distribution-discriminator to differentiate between human and task-predictor solutions. At inference for a new task, the task-predictor can be adapted to produce an initial solution for inference-time reasoning in the System II module, while the distribution-discriminator can be adapted to reward refinement of solutions towards the direction of correct solutions. This adaptation uses a small number of human-labelled samples (8-16 in our experiments) to adapt both the task-predictor and distribution-discriminator prior to System II refinement to ensure task-specific predictions for the new task. The adapted distribution-discriminator in our framework is used to guide System II refinements, as it is considered more easily generalisable than the task-predictor (with higher-dimensional outputs such as pixel-level segmentation). This offers an interesting explanation for the potential performance improvement, consistent with findings from both psychology [44] (e.g. it is easy to recognise good writing vs bad but it is difficult to produce a well-written piece-of-work) and machine learning literature [45] (analogous to the discriminative-vs-generative comparison, also due to the size of solution space), as well as our own experiments (see the ‘Ablation studies’ section in supplementary materials).

The System II module aims to refine the solution for a specific sample from the target task. We implement the refinement as a flexible self-play reinforcement learning [46, 47] process, where two competing neural network agents propose refinements to an initial solution produced by the task-predictor. The distribution-discriminator scores the competing refinements by measuring the likelihood of correctness for each. The refinement with a higher score is rewarded and enacted. The competing networks are then updated, using this distribution-discriminator score-based reward, to produce progressively better competing refinements in subsequent iterations. The process repeats and the solution is iteratively refined until no further improvement is possible, as measured by the distribution-discriminator score. This iterative refinement-proposal and evaluation facilitates a dynamic improvement process where each refined solution becomes the starting point for further optimisation. This iterative self-play process thus facilitates the System II thinking module to improve solutions with added thinking time.

The final refined solution from the System II module can be used to re-train the System I module and transition tasks to fast thinking as experience grows. So, as more samples are exposed to System II thinking, the new task-specific experience of the System I module grows, which enables better initial solutions with increasing experience. This eventually reduces the time and reliance on the auto-competing System II stage. However, whether or not a task can be fully transitioned to System I, requiring no refinement in the System II stage, depends on the complexity of the task and the ability to cover task variability sufficiently. As demonstrated in the results, certain tasks may have an upper-bound of performance, which can be achieved either through extended reasoning in System II thinking or through an expansive dataset covering the

task variability. Nevertheless, complex tasks may always require System II thinking to obtain optimal performance, given finite training data unable to cover task variability.

The System II framework also models the explicit reasoning in System II thinking. Due to the iterative nature of the solution-refining System II module, the full trajectory of refinement provides a record of where and how solutions were improved, enhancing interpretability and offering insights into justifications for specific final solutions.

The framework is summarised in Fig. 3a) and 3b). Detailed methodological descriptions for implementing and training of the functions, in both modules, are presented in the ‘Methodological description’ section of the supplementary materials and open-sourced at [github.com/s-sd/system-II-vision](https://github.com/s-sd/system-II-vision).

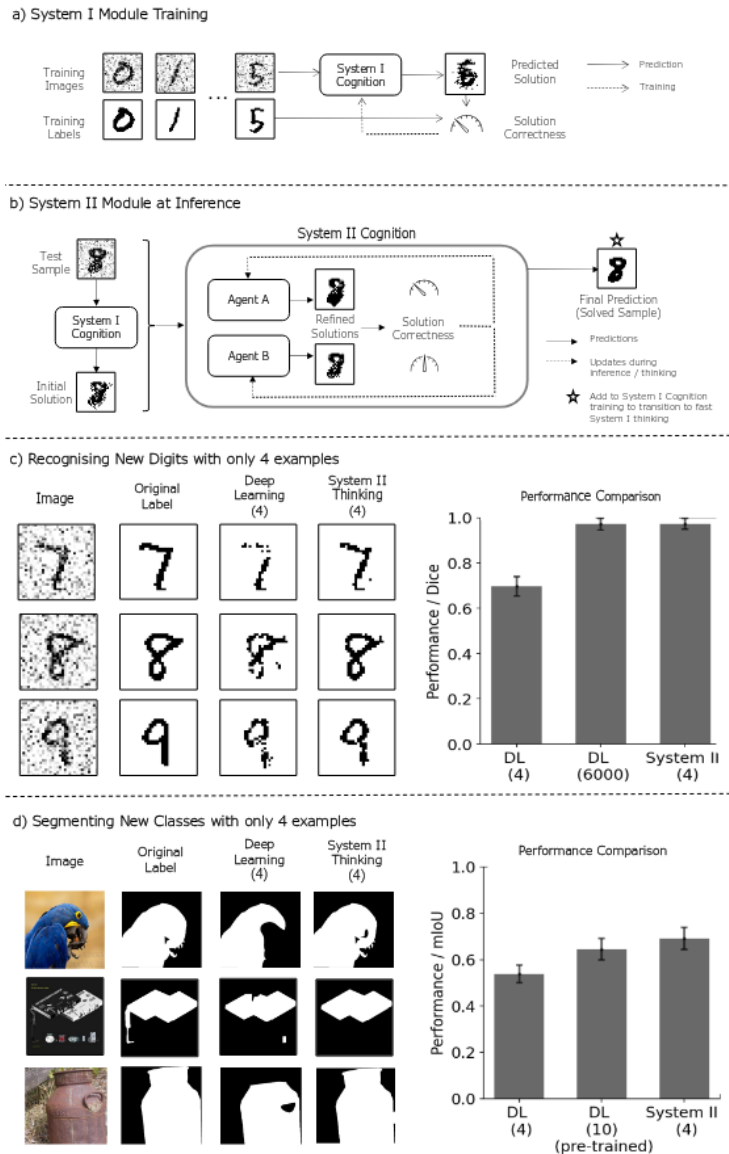


**Fig. 3:** a) and b) present an overview of the training and evaluation of the proposed System II approach. c) and d) show performance of the System II approach compared with common methods (numbers of samples used for training/ adaptation, from the target task, in brackets).

## Results

### Demonstration in standard computer vision tasks

#### *System II thinking recognises “new” digits with only four samples:*

Fig. 3a-c) illustrate how the System II method offers substantial improvement over traditional supervised learning in a simple vision task. For the task of segmenting digits

from noisy images, we trained the System I module with digits 0-5 (as shown in Fig. 3a), and then adapted this using only 4 samples from each of the unseen target digits 6-9. The System II module was then used to segment 4000 samples from each of the target digits 6-9 (as shown in Fig. 3b). Fig. 3c), shows that our dual-process approach, using extended thinking time to improve performance, substantially outperformed a deep learning algorithm (trained separately from the System I module but following a similar training scheme) [48] trained and adapted with the same data. The System II approach, using only 4 samples from the target digits, also showed similar performance to a deep learning algorithm [48] trained with 6000 samples from the target digits, representing an upper-bound performance in these new tasks.

***System II thinking significantly improves segmentation on new image classes:***

Fig. 3d) illustrates the substantially improved segmentation performance, of the System II method, on unseen real-world image classes. We trained the System I module to segment objects using 2000 images and labels randomly sampled from the ImageNet-S dataset [49]. We then adapted the System I module to segment 40 unseen target objects, using only 4 labelled samples for each. The System II module was then used to segment 6 unseen images for each of the 40 unseen objects. As shown in Fig. 3, System II thinking significantly outperformed the previous best deep-learning methods, not only when the deep learning methods used the same data, but also when they used substantially more pre-training data and labelled samples from the unseen target objects [50].

Supplementary materials section ‘detailed results for computer vision tasks’ shows that improvements offered by the System II approach were statistically significant, for both experiments above.

## Localisation of five types of abdomino-pelvic cancer

***Motivation:***

Cancer detection and localisation in medical images, such as prostate magnetic resonance (MR) and liver computed tomography (CT), holds significant promise for non-invasive diagnosis, often even outperforming the invasive alternatives [51–53]. However, democratisation of these medical imaging technologies has been severely limited by the need for highly-specialised expertise and associated costs, often only accessible in a small number of large medical centres, even in the developed countries [8, 51, 54–57]. Deep learning has been effective in segmenting anatomical structures, such as organs, where variability is relatively constrained [15, 48]. In contrast, cancer pathology presents categorically greater heterogeneity, with imaging manifestations that are less well-defined and continuously evolving due to new clinical discoveries and advancements in imaging technologies. This complexity is further compounded by the challenge of obtaining high-quality ground-truth labels, which require specialised clinical expertise or resource-intensive procedures such as independent histopathology examinations. Thus, cancer detection and localisation is a prime example where

System I cognition falls short and System II cognition may offer data-efficient performance improvements that are comparable or even superior to what expert clinicians are capable of.

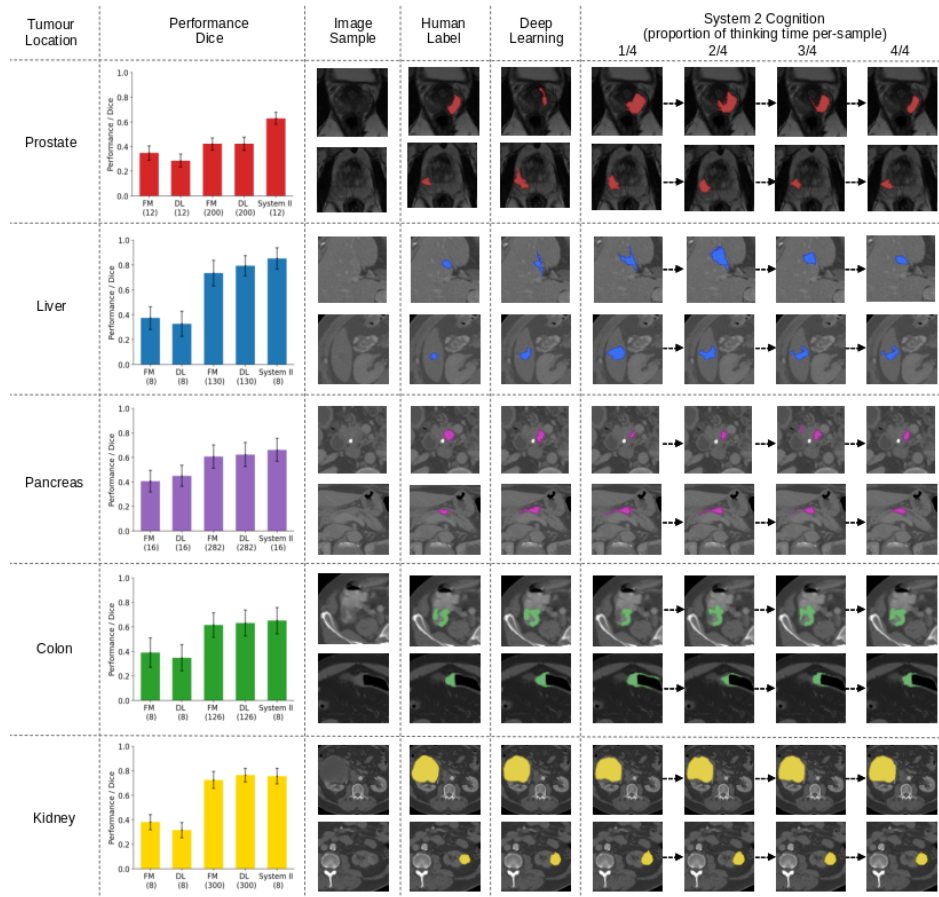


**Fig. 4:** Performance of System II thinking compared with deep learning (DL) and foundation models (FM) in five cancer localisation tasks for different organs and image types. The left column shows statistically significant increases in cancer localisation performance compared to DL and FM with equivalent training data (indicated by the numbers in brackets below), and better or at least comparable performance even when DL and FM use substantially more training data. The remaining columns provide qualitative examples demonstrating the improvement as the inference-time compute increases, further discussed in the text.

***System II thinking sets state-of-the-art performance for tested cancer localisation tasks:***

Fig. 4 shows that System II thinking achieved new state-of-the-art performance for cancer segmentation across all five distinct organs. The System I module was trained on abdomino-pelvic CT and MR images, from 955 3D human-labelled images, for over 13 anatomical structures, similar to prior work [58] (summarised in Tab. 1 in supplementary materials). This is also markedly less than the pre-training data sets required in recent image foundation models [15]. This was then adapted using few labelled samples (approximately 8-16, specified where appropriate) to the unseen target tasks of cancer localisation on medical images. The System II thinking module was evaluated for each of the five clinical tasks of localising cancer on MR or CT images from real cancer patients. Compared to the previous best methods, the System II approach outperformed (percentage points reported here) cancer segmentation in the prostate [59–62] by 20.7%, in the liver [63] by 5.9%, in the pancreas [63] by 3.9% and in the colon [63] by 2.0%, with all improvements being statistically significant (all  $p$ -values  $< 0.001$ , paired Student’s t-test at a significance level of  $\alpha=0.05$ ). It is considered equivalent to the best-performing method for kidney cancer segmentation [64]. For this task, statistical significance was not found for the comparison ( $p$ -value = 0.051), with the intra-observer [65] and inter-observer [66] variabilities reported to be high, being similar to that between human and machine segmentation [65, 66], which limit the highest measurable performance for any manual or automated segmentation method, due to the limited detectable effect size.

***System II thinking significantly outperforms foundation models:***

Fig. 4 also shows substantial improvements using System II thinking with only 8–16 labelled samples, compared to foundation models [67, 68] fine-tuned with the same or more (100-500) labelled samples. System II, using only 8-16 labelled samples, improves tumour segmentation over foundation models, using hundreds of labelled samples, by 20.9% in the prostate, 11.8% in the liver, 5.5% in the pancreas, 3.6% in the colon and 3.1% in the kidney, with all improvements being statistically significant (all  $p$ -values  $< 0.001$ ).

Numerical results for all comparisons, for cancer localisation, are presented in Table 3 in the supplementary materials.

***System II thinking outperforms radiologists with respect to independent histopathology ground-truth:***

Cancer presence in a subject can be identified through medical images and verified through an independent histopathology examination, for example, via a biopsy procedure. The classification of whether a patient has cancer or not, based on the medical image, has potential to allow non-invasive diagnoses in lieu of any invasive histology-based confirmations. Thus, for the task of classifying cancer presence in patients using only medical images, the System II approach was compared with double-blind radiologists performing the same task. The patient-wise cancer presence classifications were verified, in terms of sensitivity and specificity, against histopathology examination results. The procedure for this evaluation is outlined in ‘Retrospective evaluation

against human experts for prostate cancer detection’ in the supplementary materials. For this patient-wise classification, System II offered improved sensitivity (with 95% confidence interval) of 0.911 (0.880, 0.934) and specificity of 0.655 (0.576, 0.727) compared to the expert radiologist performance [51] with a sensitivity of 0.88 (0.84–0.91) and a specificity of 0.45 (0.39–0.51), for the same task on the same data set.

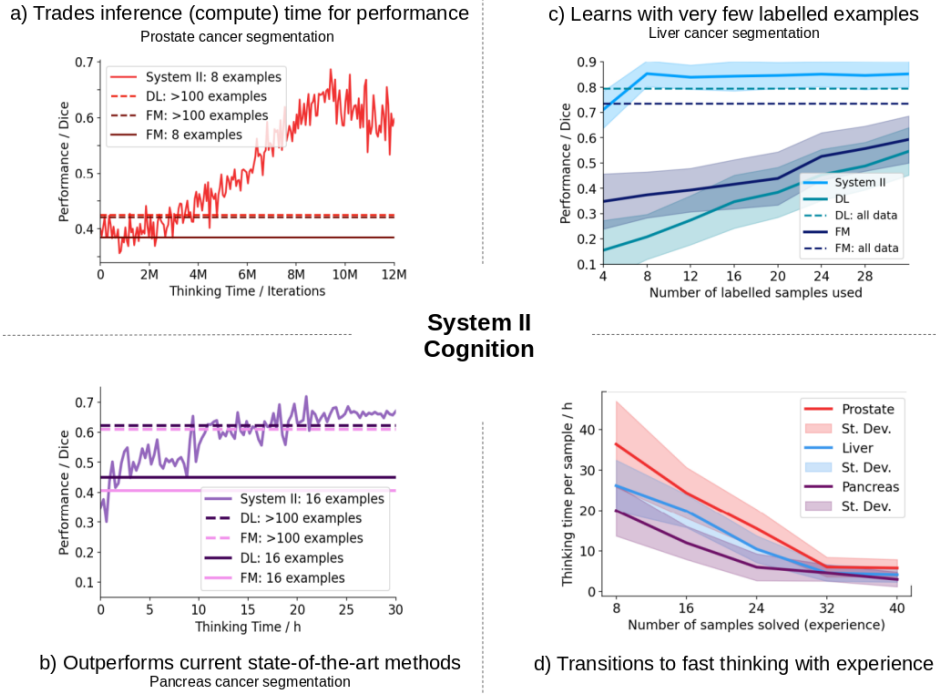


**Fig. 5:** System II thinking: a) improves performance with increasing thinking time, compared to supervised deep learning (DL) and foundation models (FM) with fixed inference time (measured in the unit of millions of optimisation iterations); b) outperforms the current best-performing deep learning (DL) methods, using substantially fewer labelled task-specific samples; c) attains peak performance with 8 labelled samples, compared to other methods requiring more than one hundred labelled samples; d) transitions tasks to fast thinking, reducing thinking time as more unlabelled samples are fully refined (or solved) by System II thinking. Performance in plotted lines is the average across 20 samples from the test set. Complete results for all cancer types can be found in the ‘Comparison to existing methods for cancer localisation’ section in the supplementary materials.

## Trading inference-time compute for machine performance

Fig. 5a-b) demonstrate a key feature of System II cognition - the ability to improve performance by utilising inference-time compute, to a much greater extent than alternative learning systems. This is shown as performance improves with a substantially longer period of increased thinking time, when we allow the System II module to auto-compete in an iterative manner, refining the solutions as the competition progresses. In this iterative refinement process, the space of performance improvement becomes much more expandable, compared with that from other single-pass or few-shot learning methods such as foundation models that have a distinct aim of being data-efficient with fixed inference time.

## Outperforming fixed-thinking-time System I approaches

Fig. 5a-b) show that the System II approach outperforms the currently best approaches in computer-vision (full details and justifications are outlined in Table 3 in the supplementary materials), which all follow a fixed-thinking-time System I paradigm. The performance improvement can be seen despite the System II approach using less than ten times the amount of data required by the solitary System I data-driven approaches.

## Learning with very few labelled samples

Fig. 5c) shows that System II thinking achieves its peak performance using only 8 labelled samples. This trend, of achieving peak performance even with a small number of labelled samples, was observed for all tested applications, for all cancer localisation tasks, with only 8-16 samples (as shown in Table 3 in the supplementary materials). We report the System II performances at their peaks and compare these, not only to other methods (deep learning and foundation models) using equivalent amounts of data, but also to their converged peak performances which require hundreds of samples.

## Transitioning from slow System II to fast System I cognition

Fig. 5d) shows the ability for the System II module to transition tasks to fast System I cognition. The System II module requires thinking time to refine solutions until no improvements are possible in the distribution-discriminator score, at which point a solution is considered fully-refined and thus solved. This solved solution is used to re-train the System I module, which enables better initial solutions, and more accurate distribution-discriminator scores, for new samples and reduces subsequent thinking time in the System II stage. The ability of reducing thinking time while maintaining the same performance, without any new human-labelled data is demonstrated in Fig. 5d), where the inference time in hours decreases as more samples are fully refined by the System II module. Note that we did not observe any cases where System II is no longer required (sufficient experience to reduce System II thinking time to zero), possibly due to the complexity and difficulty of the cancer localisation task.

## Exploring explicit reasoning in machine System II cognition

The intermediate solutions from the refinement process in System II thinking, presented in Fig. 4, show patterns of explicit reasoning in our algorithm that mimic the ability of human System II cognition. All refinements in the competition that led to higher distribution-discriminator scores, compared to the opposing lower-scoring agent, can be visualised to draw sample-specific insights and determine where and how the refinements improved solutions. As a specific example, the first row in Fig. 4 shows that the prostate gland cancerous lesion had lower intensity values and a conspicuous pattern in the peripheral zone distinct from the surrounding healthy tissue. This was challenging to identify due to close proximity of the lesion to the transitional zone which also has lower intensity compared to the peripheral zone. This may likely be the reason that the deep learning systems, without System II capabilities, deemed a significant portion of the transitional zone to be a false positive pathological region. Similar gradual local adjustments are seen in other examples, e.g., in the first sample for liver tumour segmentation where the tumour is correctly identified in System II, despite its close proximity to the falciform ligament with a similar intensity. The correct identification of only the tumour region in System II thinking, guided by the distribution scores, along with the trajectory of refinements, demonstrates its ability to overcome such challenging ambiguities in separating anatomical and pathological voxels, using inference-time refinement.

## Conclusion

The proposed dual-process framework enables performance in machine vision tasks to improve with increasing thinking time, through an iterative refinement of solutions where multiple competing solution strategies are considered before enacting the refinements - much like human thought processes. This contrasts with conventional deep learning methods, where post-training gains typically require task-specific annotations and the thinking/ inference time is fixed. In vision tasks, even recently developed foundation models and meta-learning approaches, designed for efficient data use, cannot improve through extended inference time. By contrast, System II demonstrates significant performance gains in real-world vision tasks such as cancer detection on medical images, purely by increasing thinking time. This highlights the potential to automate many challenging tasks through inference-time compute strategies, particularly when large amounts of labelled data are expensive or impossible to obtain, e.g., in data-scare domains such as rare disease identification and galaxy classification in astronomy. With compute power becoming more readily accessible, such approaches have potential to improve a variety of challenging real-world tasks, potentially even when large data-sets are available.

While we model System I thinking as an adaptable neural network trained across various tasks, there is potential to consider existing foundation models in this framework and improve their predictions via the proposed inference-time refinement through System II thinking. It is also noteworthy that while our competitive refinement framework for enabling System II thinking provides a general mechanism applicable to

various vision problems, some tasks may benefit from different search-based formulations or guiding inference-time compute through human feedback formulated as a reward signal.

In addition to exploring a new research direction in modelling anthropomorphic reasoning and decision-making in machines, the System II cognitive process opens a new data-efficient, performance-improving mechanism, applicable in common real-world scenarios where acquiring labelled data to improve performance may be expensive or prohibitive.

## Acknowledgments

### *Funding:*

This work was supported by the International Alliance for Cancer Early Detection, an alliance between Cancer Research UK [EDDAPA-2024/100014] & [C73666/A31378], Canary Center at Stanford University, the University of Cambridge, OHSU Knight Cancer Institute, University College London and the University of Manchester; the EPSRC grant [EP/T029404/1]; and the National Institute for Health Research University College London Hospitals Biomedical Research Centre.

### *Author contributions*

:

**S.U.S.:** Conceptualisation, data curation, formal analysis, funding acquisition, investigation, methodology, software, validation, visualisation, writing (original draft)

**Y.W.:** Validation, visualisation, writing (review and editing)

**V.K.:** Data curation, funding acquisition, resources, supervision, validation, visualisation, writing (review and editing)

**B.R.D.:** Data curation, funding acquisition, resources, supervision, validation, visualisation, writing (review and editing)

**M.J.C.:** Funding acquisition, resources, supervision, validation, visualisation, writing (review and editing)

**Y.H.:** Conceptualisation, data curation, formal analysis, funding acquisition, investigation, methodology, resources, supervision, visualisation, writing (original draft)

**D.C.A.:** Investigation, methodology, resources, supervision, visualisation, writing (review and editing)

### *Competing interests:*

The authors have no competing interests to declare.

### *Data and materials availability:*

The code and datasets are referenced in the manuscript, where appropriate, and also available at: [github.com/s-sd/system-II-vision](https://github.com/s-sd/system-II-vision).

## Supplementary materials

Methodological description  
Methodological details and definitions  
Materials and experimental details  
Supplementary results  
Fig. S6 to S7  
Algo. S1 to S2  
Tables S1 to S5  
References 69 to 84

### Methodological description

Our method emulates human dual-process cognition by integrating two distinct yet interconnected modules: the System I module, responsible for fast inference, and the System II module, designed for resource-intensive reasoning.

For the System I module, we use adversarial learning [43] to train two deep neural networks: the ‘task-predictor’ which predicts solutions to the task (such as segmenting a cat in an image), and the ‘distribution-discriminator’ which decides how likely the solution is to be ‘correct’. During training, the likelihood of the solution being correct is determined by comparing task-predictor solutions to human labels. When these networks are trained across various tasks, the respective capabilities, generating solutions and predicting correctness of these solutions, can be adapted to new tasks. In general, however, the direct prediction from task-predictor performs poorly in unfamiliar or complex scenarios, and therefore resorts to the System II module to reason about and refine solutions.

The System II module not only conducts inference-time computation to refine solutions but also updates the System I module with new insights, reducing reliance on System II for similar tasks, after the one-time inference stage that is compute-intensive. This module consists of two neural networks competing against each other by iteratively hypothesising refinements to solutions (e.g., for segmenting a dog in an image, the refinement may be a change in whether certain pixels belong to the dog or not). The initial solution comes from an adapted task-predictor from the System I module, whilst the likelihood of the refinements being correct in the competing process is predicted by the adapted distribution-discriminator. The initial solution is refined until no further improvement in the likelihood of the solution being correct is possible, at which point the sample is considered ‘solved’. The solved samples are used to update the System I module, which can then better and much more efficiently predict solutions for similar future tasks. This approach mimics human cognition which commits new scenarios to memory, reducing System II thinking time for future tasks. With sufficient experience, tasks may fully transition to System I, where System II thinking may no longer be required.

We present a mathematical formulation for our method in the following subsections. An overview is presented in Fig. 6.

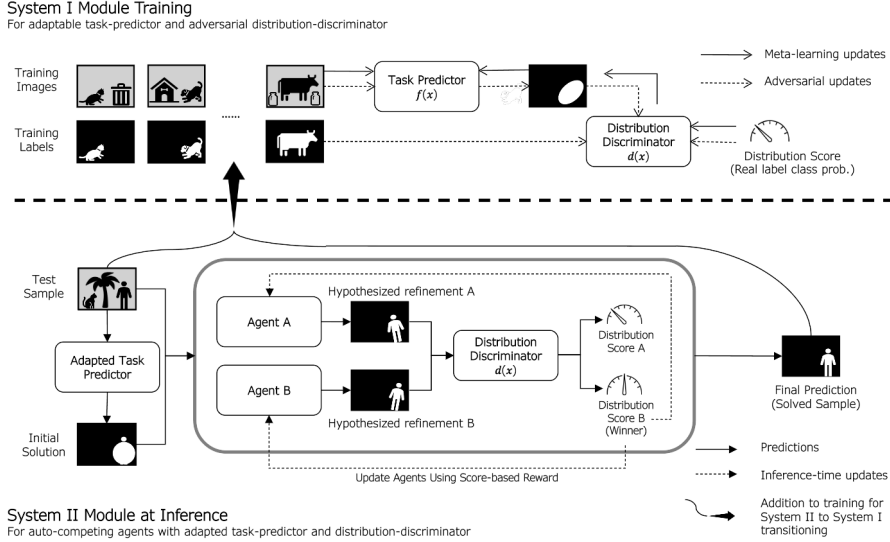


**Fig. 6:** An overview of the dual process approach, with the data flow and functions summarised for a target task of human segmentation on images.

## The System I module - for adaptable initial solutions and distribution scoring

Without loss of generality assume that an image sample  $x \in \mathcal{X}$  has a human label  $y_h \in \mathcal{Y}_h$  (e.g., a binary image mask to delineate an object’s boundaries), with  $\mathcal{X}$  and  $\mathcal{Y}_h$  denoting the image and human label distributions, respectively.

The **task-predictor**  $f(x; w) = y_t : \mathcal{X} \rightarrow \mathcal{Y}_t$ , with network weights  $w$ , aims to approximate the human label  $y_h \in \mathcal{Y}_h$ , where the task-predictor’s output label prediction belongs to the task-predictor label distribution denoted as  $y_t \in \mathcal{Y}_t$ .

The **distribution-discriminator**  $d(x, y; \theta) = \hat{z} : \mathcal{X} \times (\mathcal{Y}_h + \mathcal{Y}_t) \rightarrow [0, 1]$ , with network weights  $\theta$ , predicts a score  $\hat{z} \in [0, 1]$  between 0 and 1 given an image-label pair  $(x, y)$ , where  $y \in \mathcal{Y}_h + \mathcal{Y}_t$  may be from either the human  $\mathcal{Y}_h$  or task-predictor  $\mathcal{Y}_t$  label distributions. A score of zero indicates the pair being from the task-predictor label distribution  $\mathcal{Y}_t$ , and a score of 1 indicates the pair being from the human label distribution  $\mathcal{Y}_h$ , i.e.  $z = 0$  if  $y \in \mathcal{Y}_t$  and  $z = 1$  if  $y \in \mathcal{Y}_h$  where  $z \in \{0, 1\}$  is its random variable representing the distinction between human and task-predictor labels.

**Adversarial training** is used to train the two networks. Let  $\mathcal{L}(\cdot) : \mathbb{R}^1 \times \mathbb{R}^1 \rightarrow \mathbb{R}^1$  be a function that measures the difference between the distribution-discriminator prediction  $\hat{z}$  and the underlying distribution score label  $z$ . The distribution-discriminator can thus learn to distinguish between task-predictor and human labels. The optimal weights of the distribution-discriminator,  $\theta^*$ , can be obtained by solving the following optimisation problem, using human labels as well as task-predictor labels:

$$\theta^* = \arg \min_{\theta} \mathbb{E}_{x \sim \mathcal{X}, y \sim \mathcal{Y}_h + \mathcal{Y}_t} [\mathcal{L}(z, \hat{z})], \quad (1)$$

where  $\hat{z} = d(x, y; \theta)$ .

Note that the loss function for optimising Eq. 1 that measures the difference between two real numbers is defined as  $\mathcal{L}(\cdot) : \mathbb{R}^1 \times \mathbb{R}^1 \rightarrow \mathbb{R}^1$ , where it takes the form:

$$\mathcal{L}(a, b) = -[a \times \log(b)] - [(1 - a) \times \log(1 - b)] \quad (2)$$

The task-predictor learns to approximate human labels by minimising the difference between the distribution scores of the task-predictor  $\hat{z}$  and the distribution scores for human labels (i.e., 1), by updating the task-predictor weights towards the optimal weights  $w^*$ , in the following optimisation problem:

$$w^* = \arg \min_w \mathbb{E}_{x \sim \mathcal{X}} [\mathcal{L}(1, \hat{z})], \quad (3)$$

where  $\hat{z} = d(x, y_t; \theta)$ ,  
and  $y_t = f(x; w)$ .

In a practical algorithm, the distribution- and task-predictor weight-updating steps are iterated alternatively, until equilibrium [43].

In our work, we assume that during training, the image  $x \in \mathcal{X}$  is sampled from a distribution of abdominal CT or MR images, and the human-label  $y \in \mathcal{Y}_h$  is a segmentation label, where segmentation tasks include various organ and region-of-interest segmentation tasks. Training across a variety of tasks [45] ensures that the task- and distribution-discriminators are generalisable to other tasks on abdominal CT or MR images, during inference. We use the Reptile algorithm [45] for meta-learning across various tasks as outlined in Algo1.

After training the System I module, this can be **adapted to new tasks** (following Eq. 1 and 2), that did not form part of the training data. This step enables the System I module to output better initial solutions (to be refined by the System II module) and more accurate distribution-discriminator scores, for the new task. This can be achieved using a few human-labelled samples (between 4-16 in our experiments) and following the same update procedure as in training (following Eq. 1 and 2 and Algo. 1, with details on convergence outlined in the Methodological details and definitions section). Then, the adapted task-predictor predicts labels for the new task, for a new sample  $x_n$ , following  $f(x_n; w^*) = y_{t,n}$ . The distribution score  $\hat{z} \in [0, 1]$  for this particular sample can be computed using the adapted distribution-discriminator  $\hat{z} = d(x_n, y_{t,n}; \theta^*)$ .

### Algorithm for training and adapting the System I module

We propose to train the System I module across various tasks such that it is adaptable to any new tasks with limited labelled samples. This is achieved by employing the

Reptile algorithm during training as summarised in Algo. 1. We can define sample  $(x^j, y^j)$  as coming from task  $j$ , with a total of  $J$  tasks available during training.

---

**Data:**  $N$  image-label pairs from each of  $J$  tasks  $\{\{x_n^j, y_{h,n}^j\}_{n=1}^N\}_{j=1}^J$   
**Result:** Trained distribution-discriminator  $d(\cdot; \theta^*)$  and task-predictor  $f(\cdot; w^*)$

---

```

while not converged do
  Randomly sample a task  $j \in [1, J]$ 
  For task  $j$ , randomly sample  $B$  image-label pairs  $\{x_n^j, y_{h,n}^j\}_{n=1}^B$ 
  for  $k \leftarrow 1$  to  $K$  do
    Compute task-predictions  $f(x_n; w)_{n=1}^B = y_{t,n=1}^B$ 

    Combine human and task-predictor labels
     $\{y\}_{n=1}^{2B} = \{y_{h,n}\}_{n=1}^B \cup \{y_{t,n}\}_{n=1}^B$ 
    Get corresponding underlying distribution scores
     $\{z\}_{n=1}^{2B} = \{1\}_{n=1}^B \cup \{0\}_{n=1}^B$ 
    Assemble image samples  $\{x\}_{n=1}^{2B} = \{x\}_{n=1}^B \cup \{x\}_{n=1}^B$ 

    Compute distribution-predictions  $\hat{z}_{n=1}^{2B} = d(x_n, y_n; \theta)_{n=1}^{2B}$ 
    Take one step of gradient descent to get  $\theta_{new}$  following
     $\arg \min_{\theta} \mathbb{E}_{x, y} [\mathcal{L}(z, \hat{z})]$ 
    Update  $\theta \leftarrow \theta + \epsilon(\theta_{new} - \theta)$ 

    Compute new distribution-predictions  $\hat{z}_{n=1}^B = d(x_n, y_{t,n}; \theta)_{n=1}^B$ 
    Take one step of gradient descent to get  $w_{new}$  following
     $\arg \min_w \mathbb{E}_x [\mathcal{L}(1, \hat{z})]$ 
    Update  $w \leftarrow w + \epsilon(w_{new} - w)$ 
  end
end

```

---

**Algorithm 1:** Training an adaptable System I module

The same scheme as Algo. 1 can be used to adapt the System I module to a new task, in which only the new task is sampled, instead of randomly sampling a task from  $J$  tasks.

## The System II module - for an iterative competition between solution refinements

### *Initial solution using the System I module:*

The System II module aims to refine the task-predictor label  $y_{t,n}$  for a new sample  $x_n$ . Since the System II module does not involve any human labels, and works on a per-sample basis, we now omit the subscripts  $t$  and  $n$  from  $y_{t,n}$ , in favour of the notationally convenient  $y$ , to aid readability. So before conducting System II thinking for a new sample  $x$ , we first compute an initial solution using the System I task-predictor  $y = f(x; w^*)$ .

### *Competing solution refinement functions:*

The auto-competing process in System II thinking involves two competing functions that iteratively refine the task-predictor label. Since the process is iterative, we use a subscript  $i$  to denote the iteration number. The competing function is denoted as  $h(x, y_i; \phi) = y_{i+1} : \mathcal{X} \times \mathcal{Y}_t \rightarrow \mathcal{Y}_t$ , with weights  $\phi$ , where both the pre-refinement label  $y_i$  and post-refinement label  $y_{i+1}$  are assumed to belong to the task-predictor distribution  $y_i, y_{i+1} \in \mathcal{Y}_t$ , even though the actual distribution of refined labels may be different from the task-predictor label distribution. Since there are two competing functions  $a$  and  $b$  we can denote the two competitors as  $h(\cdot; \phi_a)$  and  $h(\cdot; \phi_b)$ , with the only difference between the two being the function weights. In practice, weights  $\phi_b$  are either a copy of  $\phi_a$ , or  $\phi_b$  are sampled from a distribution over all historical weights during training and the weights  $\phi_a$  are the most up-to-date weights during training (see further implementation details in ‘Methodological details and definitions’ section).

### *Optimising the competitors during the auto-competing process:*

Starting with a new sample  $x$  and its task-predictor label  $y$  at iteration  $i = 0$ , both competitors refine the label  $h(x, y_i; \phi_a) = y_{i+1,a}$  and  $h(x, y_i; \phi_b) = y_{i+1,b}$ ; here, and in further analyses, subscripts of  $a$  or  $b$  denote outputs from competitors  $a$  or  $b$ , respectively. The distribution score is measured for both refined labels  $d(x, y_{i+1,a}; \theta^*) = \hat{z}_{i,a}$  and  $d(x, y_{i+1,b}; \theta^*) = \hat{z}_{i,b}$ . These distribution scores are used to formulate a reward for competitor  $a$ :

$$R_i = \begin{cases} +1 & \text{if } \hat{z}_{i,a} \geq \hat{z}_{i,b} \\ -1 & \text{otherwise} \end{cases} \quad (4)$$

This reward is used to train both competitors and update weights  $\phi$  towards optimal weights  $\phi^*$ . For the next iteration  $i = i + 1$ , the refined solution with the higher distribution-discriminator score is set as  $y_{i+1}$ , meaning that we only use the winning refinement to further refine in the next iterations. We allow iteration of this process until a maximum iteration number  $i_{end}$  (see ‘Methodological details and definitions’ for procedure of computing the value of  $i_{end}$ ). We can then reset the refinements and repeat the iterative refinement to collect multiple sets of  $[R_i]_{i=0}^{i_{end}}$ . The optimisation

of weights  $\phi$ , using experience from both competing sides, can be formulated as the following optimisation problem over multiple collected sets of rewards:

$$\phi^* = \arg \max_{\phi} \left[ \mathbb{E}_{y_{i,a} \sim h(\cdot; \phi_a)} \left[ \sum_{i=0}^{i_{end}} R_i \right] + \mathbb{E}_{y_{i,b} \sim h(\cdot; \phi_b)} \left[ \sum_{i=0}^{i_{end}} -R_i \right] \right] \quad (5)$$

Solving the above optimisation problem for a single sample  $x$  means that no further improvements in the distribution score are possible and thus the fully-refined sample is considered as solved by the System II thinking module. This reward-based training is known as reinforcement learning self-play [46, 47], where competitors start out with random behaviours which are then refined towards maximising the reward. Practically it may be beneficial to aggregate updates to the competitor weights across a few different samples (up to 8 tested in our experiments), to ensure stable training [69–71]. As opposed to directly optimising the task-predictor using the distribution score for a single new sample e.g., using the adversarial training framework to model System II, our auto-competing process which incorporates exploration by the use of reinforcement learning, ensures that the optimisation does not get stuck in local optima, which is a common problem with other adversarial learning frameworks [43, 72–74].

### Transitioning tasks from System II to System I

After a sample is solved by System II thinking, it can be used to update the System I module using the refined label in-place of the human label (following Eq. 1 and 2) to allow the next sample to get a better initial task-predictor label, to reduce the System II thinking time for the subsequent samples. In practice, similar to aggregating updates to the competitor, updates to the System I module can also be aggregated across a few (8 in our experiments) different samples.

### Algorithm for the auto-competing process

The auto-competing process is initialised by first obtaining an initial solution from the already-trained task-predictor. This is then refined by both competitors in the auto-competing process. The distribution scores are computed for both refined solutions and then the one leading to a higher score wins the iteration and is selected to be used for the next iteration. On the next iteration, the refined solution is then further refined by both competitors and the entire process is repeated. Once a specified number of iterations have elapsed, we can update the competitors using gradient ascent informed by the win or loss of the iteration, formulated into a reward. Resetting the refinements and repeating these updates until convergence, we eventually obtain an optimal refinement strategy that leads to the highest distribution score. Then the sample is considered as solved by the System II thinking. This process is summarised in Algo. 2.

---

**Data:** New sample image  $x$   
**Result:** Optimal refinement strategy  $h(\cdot; \phi^*)$

---

Set  $H = 0$

**while** *not converged* **do**  
  Start at  $i = 0$   
  Sample an initial solution using the task-predictor  $f(x; w^*) = y$   
  
  Set competitor  $a$  weights to  $\phi_{a,H}: h(\cdot; \phi_{a,H})$   
  Set competitor  $b$  weights to  $\phi_{b,H_s}: h(\cdot; \phi_{b,H_s})$   
  
  Sample initial refinement for competitor  $a$ :  $y_{i=0+1,a} = h(x, y; \phi_{a,H})$   
  Sample initial refinement for competitor  $b$ :  $y_{i=0+1,b} = h(x, y; \phi_{b,H_s})$   
  
  Compute competitor  $a$  distribution score:  $d(x, y_{i=0+1,a}; \theta^*) = \hat{z}_{i=0+1,a}$   
  Compute competitor  $b$  distribution score:  $d(x, y_{i=0+1,b}; \theta^*) = \hat{z}_{i=0+1,b}$   
  
  Compute reward  $R_1$  using eq 4  
  
  **If:**  $\hat{z}_{i=0+1,a} \geq \hat{z}_{i=0+1,b}$ , **Then:** Set  $y_{i+1} = y_{i=0+1,a}$  **Else:** Set  
    $y_{i=0+1} = y_{i=0+1,b}$   
  
  **for**  $i \leftarrow 1$  **to**  $i_{end}$  **do**  
   Sample initial refinement for competitor  $a$ :  $y_{i+1,a} = h(x, y_i; \phi_{a,H})$   
   Sample initial refinement for competitor  $b$ :  $y_{i+1,b} = h(x, y_i; \phi_{b,H_s})$   
  
   Compute competitor  $a$  distribution score:  $d(x, y_{i+1,a}; \theta^*) = \hat{z}_{i+1,a}$   
   Compute competitor  $b$  distribution score:  $d(x, y_{i+1,b}; \theta^*) = \hat{z}_{i+1,b}$   
  
   Compute reward  $R_{i+1}$  using eq 4  
  
   **If:**  $\hat{z}_{i+1,a} \geq \hat{z}_{i+1,b}$ , **Then:** Set  $y_{i+1} = y_{i=0+1,a}$  **Else:** Set  
     $y_{i=0+1} = y_{n,i=0+1,b}$   
  **end**  
  Once  $R_{i=1:i_{end}}$  collected, update weights  $\phi$  using Eq. 5  
  Set  $H = H + 1$   
**end**

---

**Algorithm 2:** System II solution refinement through and auto-competing mechanism

## Methodological details and definitions

### Competitor sampling

As outlined in Algo. 2, the variable  $H$  is iterated every-time the competitor weights are updated. The weights of competitor  $a$  are set to  $\phi_{a,H}: h(\cdot; \phi_{a,H})$ , meaning that these remain as the most up-to-date weights in the optimisation process. However, the weights of competitor  $b$  are set to  $\phi_{b,H_s}: h(\cdot; \phi_{b,h})$  where in the simplest case  $H_s = H$  which is commonly known as vanilla reinforcement learning self-play [47]. In our work, we use fictitious self-play to avoid the optimisation being stuck in solutions that do not improve [47], which means that  $H_s \sim 1/H$ , denoting the sampling of  $H_s$  from a uniform distribution of all values between 0 and  $H$ . Practically this means that competitor  $b$  is a historic version of competitor  $a$  with weights for competitor  $a$  sampled from a uniform distribution of all historic weights of competitor  $a$ .

### The definition of ‘refinement’

Assuming that a grey-scale image  $x \in \mathbb{R}^P$  has  $P$  pixels, we can assume that the segmentation for such an image would take the form  $y \in \{0, 1\}^P$ . The refinement of this segmentation that we have thus far summarised as  $y_{i+1} = h(x, y_i; \phi)$  can then be modelled in a number of steps as follows:

The refinement  $y_{i+1} = h(x, y_i; \phi)$  is broken down as follows :

A segmentation label is denoted as:  $y_i \in \{0, 1\}^P$

In actuality  $h(x, y_i; \phi) = q \in [0, 1]^P$ , values between 0 and 1;

For  $q \in [0, 1]^P$  set top  $p$  values to 1 and rest to 0, to get:  $q_{rounded} \in \{0, 1\}^P$

Apply refinement as an element-wise logical **XOR** operation:  $y_{i+1} = y_i \oplus q_{rounded}$

This refinement is carried out using fixed parameters in our work, which were set based on a grid search across 5 different applications. In our work,  $p = 0.01$  and  $i_{end} = p \times P \times 100$ .

### The definition of convergence

The convergence in the context of training the System I module is evaluated with respect to the loss  $\mathcal{L}$ . Let iterations in the while loop in Algo 1 be denoted as  $o$ . The loss at iteration  $o$  can thus be denoted as  $L_o$ . The convergence criterion is defined based on the change in windowed moving average across iterations:

$$1/10 \left[ \sum_{v=0}^{10-1} L_{o-v} - \sum_{v=0}^{10-1} L_{o-10-v} \right] \leq 1e-5 \quad (6)$$

The System II module is considered as converged when the value of  $R_i$  stabilises. We can first define  $R_{sum} = \sum_{i=1}^{i_{end}} R_i$ . Since we iterate  $H$  every time  $R_{i=1:i_{end}}$  is collected, we can use  $H$  as a subscript denoting the sum of rewards at iteration  $H$  as  $R_{sum, H}$ . The convergence criterion is then defined as:

$$1/10 \left[ \sum_{v=0}^{10-1} R_{sum, H-v} - \sum_{v=0}^{10-1} R_{sum, H-10-v} \right] \leq 1 \quad (7)$$

## Materials and experimental details

### Datasets

For pre-training the System I module, we used a collection of data sets following previous work [58], as outlined in Tab. 1. All included data sets are considered relevant to the abdomino-pelvic region and thus the System I learns to be adaptable to other structures or pathologies in the abdomino-pelvic region. The subsequent adaptation to the target task required 8-16 samples.

For data sets that were used for evaluation, we split the data sets, on subject level, into a ratio of 60:40 for the development and held-out sets, to ensure sufficient statistical power for validation. For training or adaptation, we randomly sampled data from the development sets. All results are reported on the held-out sets.

Dataset	Modality	Structure	Cohort Country	Samples (Held-Out)	Role
[75]	CT	Spleen	United States	41	Training
[75]	CT	Liver Vessels	United States	303	Training
[76]	CT	Gallbladder	United States	30	Training
[76]	CT	Adrenal Gland	United States	30	Training
[76]	CT	Major Vessels	United States	30	Training
[76]	CT	Stomach	United States	30	Training
[77]	CT	Kidneys	>3 countries	119	Training
[77]	CT	Bladder	>3 countries	119	Training
[78]	MR	Liver	Turkey	15	Training
[78]	MR	Kidneys	Turkey	15	Training
[78]	MR	Spleen	Turkey	15	Training
[79]	MR	Bladder	China	40	Training
[79]	MR	Gallbladder	China	40	Training
[79]	MR	Prostate	China	40	Training
[79]	MR	Major Vessels	China	40	Training
[75]	MR	Prostate	Netherlands	48	Training
[80]	mp-MR	Prostate Tumour	United Kingdom	520 (208)	Evaluation
[75]	CT	Liver Tumour	France	131 (52)	Evaluation
[75]	CT	Pancreas Tumour	United States	282 (112)	Evaluation
[75]	CT	Colon Tumour	United States	126 (50)	Evaluation
[81]	CT	Kidney Tumour	United States	489 (195)	Evaluation

**Table 1:** A summary of the data sets used for training and evaluation.

### Network architectures and hyper-parameters

The hyper-parameters, including the network architectures used are summarised in Tab. 2.

Task-Predictor - UNet [48]	
Input Size	256 × 256
Batch Size $B$	64
Optimiser	Adam
Reptile $\epsilon$	0.02
Distribution-discriminator - ResNet38	
Input Size	256 × 256
Batch Size	64
Optimiser	Adam
Competing Refinement Functions - UNet [48]	
Input Size	$P = 256 \times 256$
Batch Size	8
Optimiser	Adam
Proportion of pixels to flip per iteration $p$	$p = 0.01$
Terminal Iteration $i_{end}$	$p \times P \times 100$

**Table 2:** A summary of hyper-parameter configurations used in this work.

## Supplementary results

### Detailed results for computer vision tasks

#### *Digit segmentation from noisy images*

For the MNIST digit classification dataset we added Gaussian noise to the images, and thresholded the original clean images at an intensity of 0.5 to generate segmentation ground-truth labels. The System I module was trained to segment digits from noisy images using digits 0–5. System II thinking, implemented through our proposed framework, was then applied to segment the remaining digits 6-9 (refer to the open-source code repository for further details). For each of the unseen target digits, we used four samples to adapt the System I module prior to System II thinking.

To evaluate performance, we tested the model on 4000 samples of these digits (i.e., digits 6-9). As shown in Fig. 3, we observed dramatic performance improvements (p-value= 0.0002, paired Student’s t test at a significance level of  $\alpha = 0.05$ ) compared to supervised deep learning [48] using the same training and adaptation data as our System II approach. Our proposed System II module achieved a Dice score of  $97.3 \pm 2.4$ , compared with the deep learning models which achieved  $69.7 \pm 4.3$  and  $97.2 \pm 2.6$ , when using 4 and 6000 samples from the target digits for learning, respectively. The latter is an upper-bound performance for these new tasks.

#### *Object segmentation for new classes*

Out of 919 classes in the ImageNet-S large-scale unsupervised semantic segmentation (LUSS) data set [49], we reserved 40 randomly sampled classes to evaluate our approach. Ten images were randomly sampled from each of these 40 reserved classes (for the purpose of this study, only those classes are considered if they have at least 10 images available per-class). From the remaining classes, ensuring none of the reserved held-out classes were present, 2000 training images were randomly sampled, to train the System I module across different classes, to predict the segmentation of objects.

For each of the 40 reserved classes, the System I module was adapted using 4 samples and evaluation was done on the remaining 6 samples. For these  $40 \times 6 = 240$  samples, we generated segmentations using our System II thinking approach.

As shown in Fig. 3, our approach obtained a mean intersection over union (mIoU) of  $0.691 \pm 0.047$  compared to the previous best-performing method [50] that obtained  $0.538 \pm 0.039$  mIoU when using the same training and adaptation data as our System II approach, or  $0.645 \pm 0.046$  mIoU when using the pre-training strategy as outlined in [50] (p-values = 0.0006 and 0.003, respectively).

### **Comparison to existing methods for cancer localisation**

In Tab. 3, we present detailed results for cancer detection tasks, comparing our System II approach to not only the previous best-performing specialised deep learning models but also to foundation models and widely-used benchmarking U-Nets. The amount of human-labelled data used for training of each method is investigated. Methods that have been pre-trained refer to those using other tasks for learning as summarised in Tab. 1, with the Reptile algorithm [45] being used to pre-train across these different tasks. Our method shows superior performance compared to the previously best-performing methods as well as to foundation models and specialised U-Nets trained with much larger datasets (in the order of hundreds of samples), compared to our method which only uses 8-16 samples from the target task.

### **Retrospective evaluation against human experts for prostate cancer detection**

We evaluate performance against uro-radiology-specialised radiologists in prostate cancer detection, in which ground-truth labels are available from independent histopathology examinations. We trained our System II cognition using 16 samples with histopathology labels derived from prostate template-mapping biopsy to indicate cancer presence in one of the twenty Barzell zones within the gland [51]. Each zone had a label of one to indicate positive cancer with a Gleason grade  $\geq 3+4$ , and zero otherwise. We observed an across-zone sensitivity and specificity of 0.774 and 0.582. From the zonal predictions, we predicted patient-wise classification (by predicting cancer presence when any single zone was deemed cancer-positive). We used zonal prediction to compute patient-wise classification, as zonal prediction can be formulated as low-resolution segmentation and thus does not require retraining of the System I module for classification tasks, in addition to its potential spatial interpretability.

### **Ablation studies**

For the task of liver tumour segmentation, we also present ablation studies in Tab. 4, where we remove components including adversarial training and RL from our framework to evaluate their impact on task performance. When adversarial training is omitted, the two networks in the System I module are trained separately, where the task-predictor is first trained to perform the task and then a distribution-discriminator is separately trained after training the task-predictor. When auto-competition is omitted, this refers to using a single agent RL framework with a reward based on

Method	Pre-Train	Labels	Prostate	Liver	Pancreas	Colon	Kidney
System II	Yes	8	62.4±5.1	<b>85.3±8.6</b>	60.9±9.7	<b>65.1±10.7</b>	<b>75.6±6.3</b>
System II	Yes	12	<b>63.0±4.8</b>	83.9±10.2	63.6±8.9	63.3±10.2	74.9±5.9
System II	Yes	16	62.8±5.8	84.3±9.1	<b>66.2±9.4</b>	64.7±11.0	74.1±6.2
UNet [48]	Yes	8	24.9±5.5	32.7±10.1	24.6±8.5	34.8±10.7	31.6±6.2
UNet [48]	Yes	12	28.5±5.3	40.2±11.3	31.2±9.2	32.4±11.6	34.1±5.3
UNet [48]	Yes	16	29.8±4.7	43.1±9.4	45.0±8.7	41.7±11.1	35.3±5.7
UNet [48]	Yes	>100	41.7±5.9	74.2±9.7	56.1±9.1	53.9±11.9	71.8±6.8
UNet [48]	No	8	18.3±5.7	20.8±8.9	20.5±9.6	28.3±11.8	30.8±6.6
UNet [48]	No	12	22.7±4.6	27.4±9.7	33.9±9.3	30.1±11.5	32.4±5.2
UNet [48]	No	16	26.8±4.9	34.7±10.5	41.4±8.5	40.9±10.3	39.3±6.3
UNet [48]	No	>100	37.6±4.9	74.5±10.4	54.0±9.9	55.2±10.2	70.2±5.6
Dv2 [67]	Yes	8	38.4±4.9	37.4±9.1	37.0±8.6	36.1±10.4	38.1±6.2
Dv2 [67]	Yes	12	37.9±4.3	39.3±8.6	37.2±8.9	37.0±10.5	37.8±5.1
Dv2 [67]	Yes	16	38.5±5.6	41.6±9.7	38.7±9.3	39.2±11.5	40.9±5.7
Dv2 [67]	Yes	>100	40.8±5.6	73.5±10.3	55.9±9.1	53.4±10.3	72.5±6.8
USeg [68]	Yes	8	27.6±5.3	-	33.2±8.2	39.1±11.9	-
USeg [68]	Yes	12	34.7±5.8	-	34.7±8.9	40.5±11.3	-
USeg [68]	Yes	16	36.0±4.7	-	40.6±8.8	42.9±10.8	-
USeg [68]	Yes	>100	42.1±5.1	-	60.7±9.5	61.5±10.1	-
nnUNet [82]	No	>100	42.3±5.6	-	-	-	-
CLIP [63]	Yes	>100	-	79.4±8.1	62.3±9.8	63.1±10.6	-
ASeg [64]	No	>100	-	-	-	-	<b>76.4±5.5</b>

**Table 3:** Cancer lesion segmentation results (Dice score, as widely reported in medical imaging literature). Where we specify > 100 human labels, the full train sets from the respective tasks have been used. **First block:** results from our System II approach; **Second block:** UNet model [48] pre-trained on the same data as our System I module using the Reptile algorithm and fine-tuned using human labels for each application; **Third block:** UNet model without pre-training; **Fourth block:** foundation models (Dv2 is DINO-v2 [67] encoder fine-tuned on 50% of training data and segmentation head fine-tuned on remaining data; with labelled samples for each application used to fine-tune the entire model before inference; USeg is the UniverSeg [68] model either fine-tuned or using support samples for each application - applications used in training of USeg were not considered); **Fifth block:** previous best-performing methods for each application. Where results are emboldened in more than one block, this indicates that statistical significance was not found for the comparison. Pre-train indicates the use of pre-training sets before training for the target task.

distribution-discriminator score, which is directly maximised, as opposed to difference in scores between the predictions from two competing agents. Where RL is omitted, the task-predictor is optimised directly per-sample by maximising the distribution-discriminator score as in the adversarial learning for each new sample. The results show that all of these components contribute positively towards performance.

### Uncertainty quantification with respect to data

To quantify the uncertainty in the computed segmentation using our proposed approach, we reserved a set of 32 samples from the liver tumour segmentation dataset. To each of these samples and their ground-truth human expert labels, we applied 32 random affine transformations. The transformations altered translation, scale, shear,

System I module			System II module		Performance
Adversarial Training	Reptile	Pre-Training	Auto-competition	RL	
✓	✓	✓	✓	✓	<b>85.3±4.3</b>
✓	✗	✗	✓	✓	57.9±5.1
✗	✓	✓	✓	✓	75.7±5.8
✓	✗	✓	✓	✓	<b>83.7±4.7</b>
✗	✗	✗	✓	✓	53.1±4.5
✓	✓	✓	✗	✓	78.5±6.3
✓	✓	✓	✗	✗	64.6±4.6
✓	✗	✗	✗	✗	38.7±4.9

**Table 4:** Ablation study - removing components from the framework to test efficacy of different approaches. The standard deviation is across different runs rather than patient cases.

rotation or a combination of these corresponding to application-specific transformations that may be observed due to shifts in imaging camera positions, variations in patient positions and variations in anatomical appearances due to noise from processes such as breathing. The standard deviation in performance (Dice score) across these affine transforms is computed per-sample and then averaged across the 32 reserved samples to obtain an estimate of the aleatoric uncertainty with respect to variations in input data.

Fig. 7 present plots of these measures of uncertainty for our proposed System II machine cognition as well as other commonly used methods for segmentation. All methods show a trend of decreasing uncertainty with an increase in the number of human labelled samples used, however, our proposed System II method shows the most stable measure of uncertainty which demonstrates its reduced reliance on human labels compared to other methods.

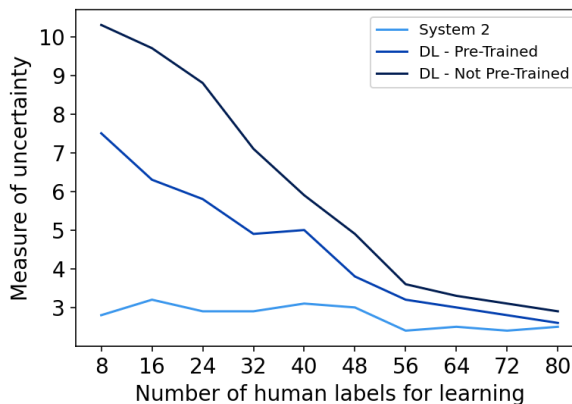


**Fig. 7:** Visualising uncertainty against number of human labelled samples used for learning, from the proposed and compared methods, in the liver tumour segmentation task.

## Computational cost

We summarise the carbon footprint of training and evaluating our proposed System II machine cognition framework in Tab. 5. For computing the total power consumption or kg of CO2 produced, the given measures can be multiplied by the GPU hours.

Hardware	GPU Hours						Power (W)	Carbon (kg CO2 / GPU hour)		
	Pre-Train	Adapt	Per-Sample Inference							
			Experience (Number of Samples)							
			0	8	16	24	32	40		
Nvidia V100	1152	16	41	36	24	16	6	6	300 W	0.13

**Table 5:** Carbon footprint for the prostate tumour segmentation task.

## Adapting the method for classification

Our System II method can readily be adapted to other machine learning tasks by modifying the definition of the solution space and its refinement. We present an example of adapting the framework to classification, which only requires a few modifications. For multi-class classification, we can reformulate the problem to multiple binary classification problems (classifying whether a sample belongs to class-of-interest or not) similar to previous work [47]. This allows labels to be standardised in the continuous range  $y \in \{0, 1\}$  for each class, which represents the class probability, with 1 being a 100% probability of belonging to the class-of-interest and 0 otherwise. To enable continuous values as labels, we apply mixup [83, 84] to training images and their labels, mixing samples from the class-of-interest with out-of-class samples. Thus the task-predictor learns to output  $f(x; w) = y \in \{0, 1\}$  for each image sample when trained adversarially.

During System II thinking, the competing function  $h(x, y_i; \phi)$  is modified to output values in the range  $\{-0.01, +0.01\}$  (instead of the flipping procedure described in the definition of refinement), which can then be added to the label  $y_i$  in order to obtain  $y_{i+1}$ . Then during System II thinking the competing functions compete to refine the class probability for the sample, which is especially useful for ambiguous samples, to assign a representative class probability.

For the classification problem, we used the same training data as the MNIST segmentation problem discussed in the preliminary results section, formed of digits 0-5. We used 4 samples to adapt the task and distribution-discriminators prior to System II thinking. For System II thinking using only the 4 samples, we observed an accuracy of 0.953, compared to 0.829 from the alternative supervised deep learning models using the same training data.

## References

- [1] Kahneman, D.: Maps of bounded rationality: Psychology for behavioral economics. *American economic review* **93**(5), 1449–1475 (2003)
- [2] Evans, J.S.B.: Heuristic and analytic processes in reasoning. *British Journal of Psychology* **75**(4), 451–468 (1984)
- [3] Kahneman, D.: Of 2 minds: How fast and slow thinking shape perception and choice [excerpt]. *Scientific American* **15** (2012)
- [4] Anthony, T., Tian, Z., Barber, D.: Thinking fast and slow with deep learning and tree search. *Advances in neural information processing systems* **30** (2017)
- [5] Evans, J.S.B.: In two minds: dual-process accounts of reasoning. *Trends in cognitive sciences* **7**(10), 454–459 (2003)
- [6] Litjens, G., Kooi, T., Bejnordi, B.E., Setio, A.A.A., Ciompi, F., Ghafoorian, M., Van Der Laak, J.A., Van Ginneken, B., Sánchez, C.I.: A survey on deep learning in medical image analysis. *Medical image analysis* **42**, 60–88 (2017)
- [7] Bhattacharya, I., Khandwala, Y.S., Vesal, S., Shao, W., Yang, Q., Soerensen, S.J., Fan, R.E., Ghanouni, P., Kunder, C.A., Brooks, J.D., *et al.*: A review of artificial intelligence in prostate cancer detection on imaging. *Therapeutic advances in urology* **14**, 17562872221128791 (2022)
- [8] Koh, D.-M., Papanikolaou, N., Bick, U., Illing, R., Kahn Jr, C.E., Kalpathi-Cramer, J., Matos, C., Martí-Bonmatí, L., Miles, A., Mun, S.K., *et al.*: Artificial intelligence and machine learning in cancer imaging. *Communications Medicine* **2**(1), 133 (2022)
- [9] Sörqvist, P., Marsh, J.E.: How concentration shields against distraction. *Current directions in psychological science* **24**(4), 267–272 (2015)
- [10] Vabalas, A., Gowen, E., Poliakoff, E., Casson, A.J.: Machine learning algorithm validation with a limited sample size. *PloS one* **14**(11), 0224365 (2019)
- [11] Wang, Y., Yao, Q., Kwok, J.T., Ni, L.M.: Generalizing from a few examples: A survey on few-shot learning. *ACM computing surveys (csur)* **53**(3), 1–34 (2020)
- [12] Ravi, S., Larochelle, H.: Optimization as a model for few-shot learning. In: *International Conference on Learning Representations* (2016)
- [13] Snell, J., Swersky, K., Zemel, R.: Prototypical networks for few-shot learning. *Advances in neural information processing systems* **30** (2017)
- [14] Kirillov, A., Mintun, E., Ravi, N., Mao, H., Rolland, C., Gustafson, L., Xiao, T., Whitehead, S., Berg, A.C., Lo, W.-Y., *et al.*: Segment anything. In: *Proceedings*

- of the IEEE/CVF International Conference on Computer Vision, pp. 4015–4026 (2023)
- [15] Ma, J., He, Y., Li, F., Han, L., You, C., Wang, B.: Segment anything in medical images. *Nature Communications* **15**(1), 654 (2024)
  - [16] Zhou, Y., Chia, M.A., Wagner, S.K., Ayhan, M.S., Williamson, D.J., Struyven, R.R., Liu, T., Xu, M., Lozano, M.G., Woodward-Court, P., *et al.*: A foundation model for generalizable disease detection from retinal images. *Nature* **622**(7981), 156–163 (2023)
  - [17] Moor, M., Banerjee, O., Abad, Z.S.H., Krumholz, H.M., Leskovec, J., Topol, E.J., Rajpurkar, P.: Foundation models for generalist medical artificial intelligence. *Nature* **616**(7956), 259–265 (2023)
  - [18] Mazurowski, M.A., Dong, H., Gu, H., Yang, J., Konz, N., Zhang, Y.: Segment anything model for medical image analysis: an experimental study. *Medical Image Analysis* **89**, 102918 (2023)
  - [19] Xie, W., Willems, N., Patil, S., Li, Y., Kumar, M.: Sam fewshot finetuning for anatomical segmentation in medical images. In: *Proceedings of the IEEE/CVF Winter Conference on Applications of Computer Vision*, pp. 3253–3261 (2024)
  - [20] Li, K., Rajpurkar, P.: Adapting segment anything models to medical imaging via fine-tuning without domain pretraining. In: *AAAI 2024 Spring Symposium on Clinical Foundation Models* (2024)
  - [21] Guo, X., Singh, S., Lee, H., Lewis, R.L., Wang, X.: Deep learning for real-time atari game play using offline monte-carlo tree search planning. *Advances in neural information processing systems* **27** (2014)
  - [22] Silver, D., Huang, A., Maddison, C.J., Guez, A., Sifre, L., Van Den Driessche, G., Schrittwieser, J., Antonoglou, I., Panneershelvam, V., Lanctot, M., *et al.*: Mastering the game of go with deep neural networks and tree search. *nature* **529**(7587), 484–489 (2016)
  - [23] Snell, C., Lee, J., Xu, K., Kumar, A.: Scaling llm test-time compute optimally can be more effective than scaling model parameters. *arXiv preprint arXiv:2408.03314* (2024)
  - [24] Hosseini, A., Yuan, X., Malkin, N., Courville, A., Sordoni, A., Agarwal, R.: V-star: Training verifiers for self-taught reasoners. *arXiv preprint arXiv:2402.06457* (2024)
  - [25] Feng, X., Wan, Z., Wen, M., McAleer, S.M., Wen, Y., Zhang, W., Wang, J.: Alphazero-like tree-search can guide large language model decoding and training. *arXiv preprint arXiv:2309.17179* (2023)

- [26] Trinh, T.H., Wu, Y., Le, Q.V., He, H., Luong, T.: Solving olympiad geometry without human demonstrations. *Nature* **625**(7995), 476–482 (2024)
- [27] Xin, H., Ren, Z., Song, J., Shao, Z., Zhao, W., Wang, H., Liu, B., Zhang, L., Lu, X., Du, Q., et al.: Deepseek-prover-v1. 5: Harnessing proof assistant feedback for reinforcement learning and monte-carlo tree search. arXiv preprint arXiv:2408.08152 (2024)
- [28] Guo, D., Yang, D., Zhang, H., Song, J., Zhang, R., Xu, R., Zhu, Q., Ma, S., Wang, P., Bi, X., et al.: Deepseek-r1: Incentivizing reasoning capability in llms via reinforcement learning. arXiv preprint arXiv:2501.12948 (2025)
- [29] Kumar, A., Zhuang, V., Agarwal, R., Su, Y., Co-Reyes, J.D., Singh, A., Baumli, K., Iqbal, S., Bishop, C., Roelofs, R., et al.: Training language models to self-correct via reinforcement learning. arXiv preprint arXiv:2409.12917 (2024)
- [30] Wang, P., Li, L., Shao, Z., Xu, R., Dai, D., Li, Y., Chen, D., Wu, Y., Sui, Z.: Math-shepherd: A label-free step-by-step verifier for llms in mathematical reasoning. arXiv preprint arXiv:2312.08935 (2023)
- [31] Liu, R., Gao, J., Zhao, J., Zhang, K., Li, X., Qi, B., Ouyang, W., Zhou, B.: Can 1b llm surpass 405b llm? rethinking compute-optimal test-time scaling. arXiv preprint arXiv:2502.06703 (2025)
- [32] Lightman, H., Kosaraju, V., Burda, Y., Edwards, H., Baker, B., Lee, T., Leike, J., Schulman, J., Sutskever, I., Cobbe, K.: Let’s verify step by step. arXiv preprint arXiv:2305.20050 (2023)
- [33] Uesato, J., Kushman, N., Kumar, R., Song, F., Siegel, N., Wang, L., Creswell, A., Irving, G., Higgins, I.: Solving math word problems with process-and outcome-based feedback. arXiv preprint arXiv:2211.14275 (2022)
- [34] Weston, J., Sukhbaatar, S.: System 2 attention (is something you might need too). arXiv preprint arXiv:2311.11829 (2023)
- [35] Cormen, T.H., Leiserson, C.E., Rivest, R.L., Stein, C.: *Introduction to Algorithms*. MIT press, ??? (2022)
- [36] Wei, J., Wang, X., Schuurmans, D., Bosma, M., Xia, F., Chi, E., Le, Q.V., Zhou, D., et al.: Chain-of-thought prompting elicits reasoning in large language models. *Advances in neural information processing systems* **35**, 24824–24837 (2022)
- [37] John, G.H., Kohavi, R., Pflieger, K.: Irrelevant features and the subset selection problem. In: *Machine Learning Proceedings 1994*, pp. 121–129. Elsevier, ??? (1994)
- [38] Šuch, O., Kontšek, M., Tinajová, A.: Neural pairwise classification models created

- by ignoring irrelevant alternatives. ITAT (2019)
- [39] Laakom, F., Chumachenko, K., Raitoharju, J., Iosifidis, A., Gabbouj, M.: Learning to ignore: rethinking attention in cnns. arXiv preprint arXiv:2111.05684 (2021)
  - [40] Vaswani, A.: Attention is all you need. Advances in Neural Information Processing Systems (2017)
  - [41] Su, D., Sukhbaatar, S., Rabbat, M., Tian, Y., Zheng, Q.: Dualformer: Controllable Fast and Slow Thinking by Learning with Randomized Reasoning Traces (2024). <https://arxiv.org/abs/2410.09918>
  - [42] You, S., Adap, S., Thakur, S., Baheti, B., Bakas, S.: Biochemical Prostate Cancer Recurrence Prediction: Thinking Fast & Slow (2024). <https://arxiv.org/abs/2409.02284>
  - [43] Goodfellow, I., Pouget-Abadie, J., Mirza, M., Xu, B., Warde-Farley, D., Ozair, S., Courville, A., Bengio, Y.: Generative adversarial networks. Communications of the ACM **63**(11), 139–144 (2020)
  - [44] Yun, K., Peng, Y., Samaras, D., Zelinsky, G.J., Berg, T.L.: Exploring the role of gaze behavior and object detection in scene understanding. Frontiers in psychology **4**, 917 (2013)
  - [45] Nichol, A., Achiam, J., Schulman, J.: On first-order meta-learning algorithms. arXiv preprint arXiv:1803.02999 (2018)
  - [46] Silver, D., Hubert, T., Schrittwieser, J., Antonoglou, I., Lai, M., Guez, A., Lanctot, M., Sifre, L., Kumaran, D., Graepel, T., *et al.*: A general reinforcement learning algorithm that masters chess, shogi, and go through self-play. Science **362**(6419), 1140–1144 (2018)
  - [47] Saeed, S.U., Huang, S., Ramalhinho, J., Gayo, I.J., Montana-Brown, N., Bonmati, E., Pereira, S.P., Davidson, B., Barratt, D.C., Clarkson, M.J., *et al.*: Competing for pixels: a self-play algorithm for weakly-supervised semantic segmentation. IEEE Transactions on Pattern Analysis and Machine Intelligence (2024)
  - [48] Ronneberger, O., Fischer, P., Brox, T.: U-net: Convolutional networks for biomedical image segmentation. In: Medical Image Computing and Computer-assisted intervention–MICCAI 2015: 18th International Conference, Munich, Germany, October 5–9, 2015, Proceedings, Part III 18, pp. 234–241 (2015). Springer
  - [49] Gao, S., Li, Z.-Y., Yang, M.-H., Cheng, M.-M., Han, J., Torr, P.: Large-scale unsupervised semantic segmentation. IEEE transactions on pattern analysis and machine intelligence **45**(6), 7457–7476 (2022)

- [50] Gao, S., Zhou, P., Cheng, M.-M., Yan, S.: Towards sustainable self-supervised learning. arXiv preprint arXiv:2210.11016 (2022)
- [51] Ahmed, H.U., Bosaily, A.E.-S., Brown, L.C., Gabe, R., Kaplan, R., Parmar, M.K., Collaco-Moraes, Y., Ward, K., Hindley, R.G., Freeman, A., *et al.*: Diagnostic accuracy of multi-parametric mri and trus biopsy in prostate cancer (promis): a paired validating confirmatory study. *The Lancet* **389**(10071), 815–822 (2017)
- [52] Krajewski, K.M., Pedrosa, I.: Imaging advances in the management of kidney cancer. *Journal of Clinical Oncology* **36**(36), 3582–3590 (2018)
- [53] Oliva, M.R., Saini, S.: Liver cancer imaging: role of ct, mri, us and pet. *Cancer imaging* **4**(Spec No A), 42 (2004)
- [54] Hunter, B., Hindocha, S., Lee, R.W.: The role of artificial intelligence in early cancer diagnosis. *Cancers* **14**(6), 1524 (2022)
- [55] Sprague, B.L., Conant, E.F., Onega, T., Garcia, M.P., Beaber, E.F., Herschorn, S.D., Lehman, C.D., Tosteson, A.N., Lacson, R., Schnall, M.D., *et al.*: Variation in mammographic breast density assessments among radiologists in clinical practice: a multicenter observational study. *Annals of internal medicine* **165**(7), 457–464 (2016)
- [56] Vleugels, J.L., Koens, L., Dijkgraaf, M.G., Houwen, B., Hazewinkel, Y., Fockens, P., Dekker, E.: Suboptimal endoscopic cancer recognition in colorectal lesions in a national bowel screening programme. *Gut* **69**(6), 977–980 (2020)
- [57] Czolbe, S., Arnavaz, K., Krause, O., Feragen, A.: Is segmentation uncertainty useful? In: *Information Processing in Medical Imaging: 27th International Conference, IPMI 2021, Virtual Event, June 28–June 30, 2021, Proceedings 27*, pp. 715–726 (2021). Springer
- [58] Saeed, S.U., Ramalhinho, J., Pinnock, M., Shen, Z., Fu, Y., Montaña-Brown, N., Bonmati, E., Barratt, D.C., Pereira, S.P., Davidson, B., *et al.*: Active learning using adaptable task-based prioritisation. *Medical Image Analysis* **95**, 103181 (2024)
- [59] Saeed, S.U., Yan, W., Fu, Y., Giganti, F., Yang, Q., Baum, Z., Rusu, M., Fan, R.E., Sonn, G.A., Emberton, M., *et al.*: Image quality assessment by overlapping task-specific and task-agnostic measures: application to prostate multiparametric mr images for cancer segmentation. arXiv preprint arXiv:2202.09798 (2022)
- [60] Saeed, S.U., Fu, Y., Stavrinos, V., Baum, Z.M., Yang, Q., Rusu, M., Fan, R.E., Sonn, G.A., Noble, J.A., Barratt, D.C., *et al.*: Image quality assessment for machine learning tasks using meta-reinforcement learning. *Medical Image Analysis* **78**, 102427 (2022)

- [61] Yan, W., Yang, Q., Syer, T., Min, Z., Punwani, S., Emberton, M., Barratt, D., Chiu, B., Hu, Y.: The impact of using voxel-level segmentation metrics on evaluating multifocal prostate cancer localisation. In: International Workshop on Applications of Medical AI, pp. 128–138 (2022). Springer
- [62] Pocius, M., Yan, W., Barratt, D.C., Emberton, M., Clarkson, M.J., Hu, Y., Saeed, S.U.: Weakly supervised localisation of prostate cancer using reinforcement learning for bi-parametric mr images. arXiv preprint arXiv:2402.13778 (2024)
- [63] Liu, J., Zhang, Y., Chen, J.-N., Xiao, J., Lu, Y., A Landman, B., Yuan, Y., Yuille, A., Tang, Y., Zhou, Z.: Clip-driven universal model for organ segmentation and tumor detection. In: Proceedings of the IEEE/CVF International Conference on Computer Vision, pp. 21152–21164 (2023)
- [64] Myronenko, A., Yang, D., He, Y., Xu, D.: Automated 3d segmentation of kidneys and tumors in miccai kits 2023 challenge. In: International Challenge on Kidney and Kidney Tumor Segmentation, pp. 1–7. Springer, ??? (2023)
- [65] Heller, N., Sathianathan, N., Kalapara, A., Walczak, E., Moore, K., Kaluzniak, H., Rosenberg, J., Blake, P., Rengel, Z., Oestreich, M., et al.: The kits19 challenge data: 300 kidney tumor cases with clinical context, ct semantic segmentations, and surgical outcomes. arXiv preprint arXiv:1904.00445 (2019)
- [66] Veiga-Canuto, D., Cerdà-Alberich, L., Sangüesa Nebot, C., Heras, B., Pötschger, U., Gabelloni, M., Carot Sierra, J.M., Taschner-Mandl, S., Düster, V., Cañete, A., et al.: Comparative multicentric evaluation of inter-observer variability in manual and automatic segmentation of neuroblastic tumors in magnetic resonance images. *Cancers* 14(15), 3648 (2022)
- [67] Oquab, M., Darcet, T., Moutakanni, T., Vo, H., Szafraniec, M., Khalidov, V., Fernandez, P., Haziza, D., Massa, F., El-Nouby, A., et al.: Dinov2: Learning robust visual features without supervision. arXiv preprint arXiv:2304.07193 (2023)
- [68] Butoi, V.I., Ortiz, J.J.G., Ma, T., Sabuncu, M.R., Guttag, J., Dalca, A.V.: Uni-verseg: Universal medical image segmentation. In: Proceedings of the IEEE/CVF International Conference on Computer Vision, pp. 21438–21451 (2023)
- [69] Liang, E., Liaw, R., Nishihara, R., Moritz, P., Fox, R., Goldberg, K., Gonzalez, J., Jordan, M., Stoica, I.: Rllib: Abstractions for distributed reinforcement learning. In: International Conference on Machine Learning, pp. 3053–3062 (2018). PMLR
- [70] Nair, A., Srinivasan, P., Blackwell, S., Alcicek, C., Fearon, R., De Maria, A., Panneershelvam, V., Suleyman, M., Beattie, C., Petersen, S., et al.: Massively parallel methods for deep reinforcement learning. arXiv preprint arXiv:1507.04296 (2015)

- [71] Kwok, J., Lohstroh, M., Lee, E.A.: Efficient parallel reinforcement learning framework using the reactor model. In: Proceedings of the 36th ACM Symposium on Parallelism in Algorithms and Architectures, pp. 41–51 (2024)
- [72] Creswell, A., White, T., Dumoulin, V., Arulkumaran, K., Sengupta, B., Bharath, A.A.: Generative adversarial networks: An overview. *IEEE signal processing magazine* **35**(1), 53–65 (2018)
- [73] Pan, Z., Yu, W., Yi, X., Khan, A., Yuan, F., Zheng, Y.: Recent progress on generative adversarial networks (gans): A survey. *IEEE access* **7**, 36322–36333 (2019)
- [74] Saxena, D., Cao, J.: Generative adversarial networks (gans) challenges, solutions, and future directions. *ACM Computing Surveys (CSUR)* **54**(3), 1–42 (2021)
- [75] Antonelli, M., Reinke, A., Bakas, S., Farahani, K., AnnetteKopp-Schneider, Landman, B.A., Litjens, G., Menze, B., Ronneberger, O., Summers, R.M., Ginneken, B., Bilello, M., Bilic, P., Christ, P.F., Do, R.K.G., Gollub, M.J., Heckers, S.H., Huisman, H., Jarnagin, W.R., McHugo, M.K., Napel, S., Pernicka, J.S.G., Rhode, K., Tobon-Gomez, C., Vorontsov, E., Huisman, H., Meakin, J.A., Ourselin, S., Wiesenfarth, M., Arbelaez, P., Bae, B., Chen, S., Daza, L., Feng, J., He, B., Isensee, F., Ji, Y., Jia, F., Kim, N., Kim, I., Merhof, D., Pai, A., Park, B., Perslev, M., Rezaifar, R., Rippel, O., Sarasua, I., Shen, W., Son, J., Wachinger, C., Wang, L., Wang, Y., Xia, Y., Xu, D., Xu, Z., Zheng, Y., Simpson, A.L., Maier-Hein, L., Cardoso, M.J.: The Medical Segmentation Decathlon. *arXiv* (2021)
- [76] Synapse: Multi-Atlas Labeling Beyond the Cranial Vault - Workshop and Challenge. Online; accessed Jun 2022 (2013). <https://doi.org/10.7303/syn3193805> . <https://www.synapse.org/#!/Synapse:syn3193805/wiki/217789>
- [77] Rister, B., Yi, D., Shivakumar, K., Nobashi, T., Rubin, D.L.: Ct-org, a new dataset for multiple organ segmentation in computed tomography. *Scientific Data* **7**(1), 1–9 (2020)
- [78] Kavur, A.E., Gezer, N.S., Barış, M., Aslan, S., Conze, P.-H., Groza, V., Pham, D.D., Chatterjee, S., Ernst, P., Özkan, S., *et al.*: Chaos challenge-combined (ct-mr) healthy abdominal organ segmentation. *Medical Image Analysis* **69**, 101950 (2021)
- [79] Ji, Y., Bai, H., Ge, C., Yang, J., Zhu, Y., Zhang, R., Li, Z., Zhanng, L., Ma, W., Wan, X., *et al.*: Amos: A large-scale abdominal multi-organ benchmark for versatile medical image segmentation. *Advances in neural information processing systems* **35**, 36722–36732 (2022)
- [80] Ahmed, H.U., Bosaily, A.E.-S., Brown, L.C., Gabe, R., Kaplan, R., Parmar, M.K., Collaco-Moraes, Y., Ward, K., Hindley, R.G., Freeman, A., *et al.*: Diagnostic accuracy of multi-parametric mri and trus biopsy in prostate cancer (promis): a

- paired validating confirmatory study. *The Lancet* **389**(10071), 815–822 (2017)
- [81] Heller, N., Isensee, F., Maier-Hein, K.H., Hou, X., Xie, C., Li, F., Nan, Y., Mu, G., Lin, Z., Han, M., *et al.*: The state of the art in kidney and kidney tumor segmentation in contrast-enhanced ct imaging: Results of the kits19 challenge. *Medical image analysis* **67**, 101821 (2021)
- [82] Isensee, F., Jaeger, P.F., Kohl, S.A., Petersen, J., Maier-Hein, K.H.: nnu-net: a self-configuring method for deep learning-based biomedical image segmentation. *Nature methods* **18**(2), 203–211 (2021)
- [83] Liang, D., Yang, F., Zhang, T., Yang, P.: Understanding mixup training methods. *IEEE access* **6**, 58774–58783 (2018)
- [84] Zhang, H.: mixup: Beyond empirical risk minimization. arXiv preprint arXiv:1710.09412 (2017)